

Dielectric properties of Y-doped $\text{Ba}_{1-x}\text{Sr}_x\text{TiO}_3$ ceramics

JING XU¹, HANXING LIU^{1*}, BO HE², HUA HAO¹, YIQIU LI¹, MINGHE CAO¹, ZHIYONG YU¹

¹State Key Laboratory of Advanced Technology for Materials Synthesis and Processing,
Wuhan University of Technology, 122 Luo Shi Road, Wuhan 430070, China

²SHU-Solar E PV Laboratory, Department of Physics, Shanghai University, Shanghai 200444, China

*Corresponding author: lhxhp@mail.whut.edu.cn

Y-doped $\text{Ba}_{1-x}\text{Sr}_x\text{TiO}_3$ (Y-BST) ceramics ($x = 0.1, 0.2, 0.4, 0.7$) were prepared by solid-state reaction and sintered at 1250, 1300, 1350, and 1400 °C for 1 h. The effect of strontium solution and sintering temperature on the structure, microstructure and dielectric properties of Y-BST was investigated. SEM investigations revealed a grain size decreasing with the Sr content increase. The temperature dependence of permittivity showed decrease in phase transition temperature with higher Sr content. Enhancing sintering temperature is effective to increase the grain size and improve the microstructure porosity. The XRD patterns of all Y-doped $\text{Ba}_{0.3}\text{Sr}_{0.7}\text{TiO}_3$ ceramics indicated that the crystal cell parameters increase when temperature increased. However, the (002) and (200) peaks of Y-doped $\text{Ba}_{0.3}\text{Sr}_{0.7}\text{TiO}_3$ split when sintering temperature was increased to 1400 °C, which makes the structure of the specimen transit to tetragonal ($a = 3.9857 \text{ \AA}$ and $c = 4.018 \text{ \AA}$) from cubic. It may be attributed to the fact that Y^{3+} ion can occupy both A site and B site of $\text{Ba}_{0.3}\text{Sr}_{0.7}\text{TiO}_3$ sintered at 1400 °C, which leads to the large different internal stress in individual grains, and then induces the structure change. The temperature coefficient of capacitance (TCC) value of the Y-doped $\text{Ba}_{0.3}\text{Sr}_{0.7}\text{TiO}_3$ sintered at 1400 °C changed little within $\pm 6\%$ over a temperature range from 10 to 130 °C.

Keywords: Y-doped, $\text{Ba}_{1-x}\text{Sr}_x\text{TiO}_3$ ceramics, dielectric properties.

1. Introduction

In recent years, materials with a high ε_r , dielectric constant and lead-free compositions have attracted much interest for environment-friendly applications [1, 2]. The most experimentally and theoretically investigated materials are perovskite-based SrTiO_3 , BaTiO_3 and the $\text{Ba}_{1-x}\text{Sr}_x\text{TiO}_3$ alloys, because they are prototype ferroelectrics and are used extensively in the capacitor industry [3].

Barium strontium titanate ($\text{Ba}_{1-x}\text{Sr}_x\text{TiO}_3$) is a solid solution family composed of barium titanate and strontium titanate with its Curie temperature covering a wide range of temperature. SrTiO_3 in a bulk form changes from a simple cubic perovskite structure to a tetragonal perovskite structure near 105 K and retains that phase down

to absolute zero [4]. BaTiO₃ ceramic is a typical ferroelectric material with the Curie temperature around 130 °C. BaTiO₃-based ferroelectric has been considered to be an important material for various applications, such as dynamic random access memory (DRAM) [5], multilayer ceramic capacitors (MLCCs) [6], phased array antennas [7], microwave devices [8], as well as in sensors and positive temperature coefficient (PTC) thermistor [9].

In BaTiO₃ the Curie point can be shifted to lower temperature by the substitution of Sr²⁺ for Ba²⁺, or Sn⁴⁺ or Zr⁴⁺ for Ti⁴⁺ and to higher temperatures by the substitution of Pb²⁺ for Ba²⁺ [10]. The main purpose of adding Sr²⁺ into BST is to shift the Curie temperature towards room temperature and make BST a paraelectric material at room temperature offering high dielectric constant, low leakage current and low dielectric loss against frequency.

Previous studies on the dielectric properties of Ba_{1-x}Sr_xTiO₃ ceramic solid solutions have shown that the compositions with $x < 0.2$ exhibited normal ferroelectric behaviour, while a relaxor characteristic was observed in the SrTiO₃ rich region ($x \geq 0.2$) [11, 12]. In addition, the dependence of the Curie temperature on the grain size has been reported [13]. However, knowledge of the effect of sintering temperature on the dielectric properties is still limited. In this paper, we discuss the effect of Sr²⁺ substitution and sintering condition on the dielectric properties of Ba_{1-x}Sr_xTiO₃ samples doped with 0.2 at.% Y₂O₃ (Y-BST). YUANLIANG LI *et al.* [14] reported that the proper additive amount of Y³⁺ can accelerate growth of the grains and improve the dielectric constant of Ba_{0.62}Sr_{0.38}TiO₃ ceramics. Furthermore, the authors have reported that donor doping, such as Y³⁺ for BaTiO₃-based ceramics, is an excellent method for improving the resistance degradation in highly accelerated life test (HALT) for Ni electrode MLCCs [15]. Therefore, in our experiment, the BST samples were doped with 0.2 at.% Y₂O₃.

2. Experiment

Y₂O₃ doped Ba_{1-x}Sr_xTiO₃ ceramics with molar formula ($x = 0.1, 0.2, 0.4, 0.7$) were synthesized by a solid state reaction method. The starting materials were carbonate (BaCO₃, SrCO₃) and oxide (TiO₂, Y₂O₃) powders of purity higher than 99%. The raw materials were mixed in stoichiometric proportions, ball-milled in water for 24 h, and dried in an oven. The powders were finely pulverized, precalcined and then formed into disks under a uniaxial pressure of 174 MPa. The disc-shaped pellets were sintered in air at 1250, 1300, 1350, and 1400 °C for 1 h, and furnace cooled. Silver paste was applied to both sides of the samples (1 mm thick and 10 mm diameter) and then the samples were fired at 150 °C for 1 h.

The crystalline structure of the Y-BST ceramics was analyzed by X-ray diffraction (XRD) analysis using Cu K α radiation. The microstructure and the elemental distribution were examined by scanning electron microscopy (SEM S-2500) and energy-dispersive X-ray (EDX) using a scanning electron microscope equipped with an X-ray energy-dispersive EDX spectrometer. Measurements of the temperature

dependence of the dielectric constant and dielectric loss at 1 kHz were performed on a capacitance measurement system (HP4294A), which includes a self-acting LCR bridge in the -30 to 130 °C temperature range.

3. Results and discussion

Figure 1 is the SEM images of Y-BST samples sintered at 1300 °C. It has been found that with Sr content increasing, the grain size of all specimens becomes smaller. It should be noted that the Sr^{2+} ionic radius (1.16 Å) is smaller than Ba^{2+} ionic radius (1.35 Å), so the substitution of Sr^{2+} for Ba^{2+} will make the lattice volume smaller, which suppresses the grain growth.

Figures 2a and 2b show the variation of dielectric constant ϵ_r and dielectric loss $\tan \delta$, respectively, with temperature for different samples at 1 kHz frequency performed in the -30 °C to 130 °C temperature range. The decrease in the phase transition temperature with the Sr concentration increase can be observed for all samples. The ferroelectric transition temperature of Y-BST with $x = 0.1, 0.2, 0.4$ is $110, 80$, and 10 °C, respectively. In addition, the dielectric loss ($x = 0.1, 0.2, 0.4$) also shows a peak at the transition temperature, which indicates a well-defined phase

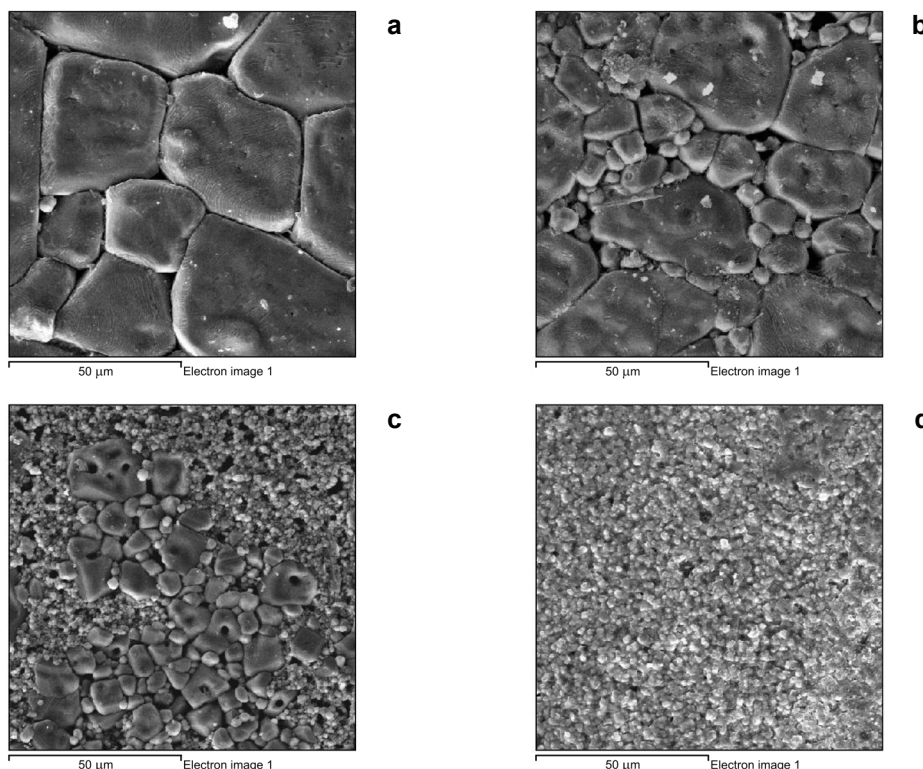


Fig. 1. SEM micrographs of Y-doped $Ba_{1-x}Sr_xTiO_3$ samples sintered at 1300 °C for 1 h; $x = 0.1$ (a), $x = 0.2$ (b), $x = 0.4$ (c), and $x = 0.7$ (d).

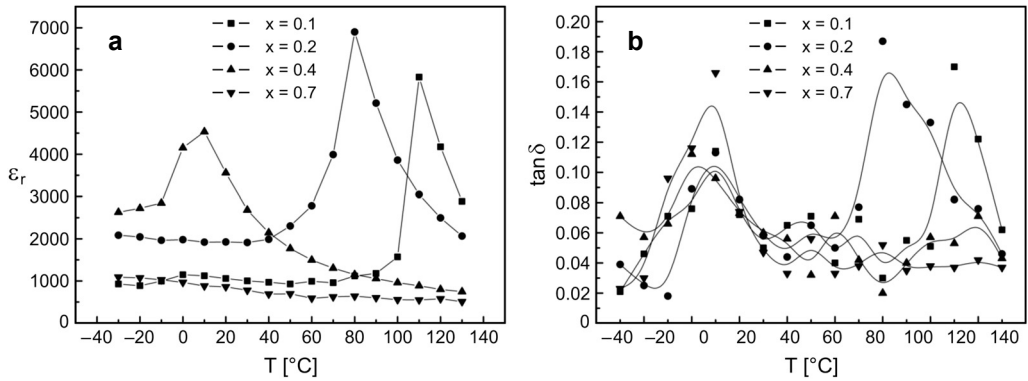


Fig. 2. Temperature variation of the dielectric constant (**a**) and dielectric loss (**b**) of Y-doped $\text{Ba}_{1-x}\text{Sr}_x\text{TiO}_3$ samples measured at 1 kHz.

transition. The dielectric constant maximum increases firstly and then decreases with Sr concentration increasing, which is due to the porosity of the structure and smaller grains seen in Fig. 1. Further, a closer look at the dielectric constant–temperature (ϵ_r-T) plots reveals a broadening of the transition peaks with higher Sr content, which can be attributed to inhomogeneous morphology and more small grains. Thanks to dielectric measurements of perovskite ferroelectrics, the diffuse phase transition can be induced by factors such as decreasing grain size and local disorder mode through the local strain [16, 17].

Figure 3 shows the XRD patterns of Y-doped $\text{Ba}_{0.3}\text{Sr}_{0.7}\text{TiO}_3$ specimens sintered at 1250, 1300, 1350, and 1400 °C for 1 h. The XRD patterns of all samples showed a single perovskite phase, which confirmed the fact that Y^{3+} ion can be almost incorporated into the perovskite lattice of BST. Moreover, the samples sintered at 1250, 1300, and 1350 °C are mainly composed of the cubic structures with lattice parameters of $a = 3.9224 \text{ \AA}$, 3.9373 \AA , and 3.9784 \AA , respectively. However, it is interesting that

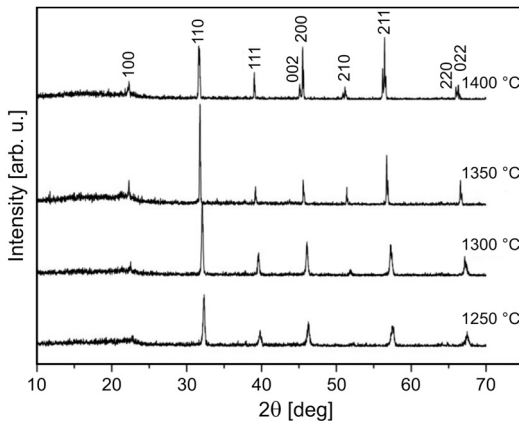


Fig. 3. XRD patterns of Y-doped $\text{Ba}_{0.3}\text{Sr}_{0.7}\text{TiO}_3$ specimens sintered at different temperatures for 1 h.

when sintering temperature increases to 1400 °C, the (002) and (200) peaks split, which implies that the structure of the specimen transiting to tetragonal ($a = 3.9857 \text{ \AA}$ and $c = 4.018 \text{ \AA}$) from cubic.

SEM images (Fig. 4) show that enhancing sintering temperature is effective to increase the grain size and microstructure density. Especially, the sample sintered at 1400 °C exhibits an exaggerated grain growth, which shows the same abnormal characteristic in the XRD analysis. This may be relative to the A or B site of Y^{3+} substitution, which is explained below.

In the ABO_3 perovskite structure, dopant cations can enter substitutionally into two different lattice sites – the smaller, octahedrally coordinated B-sites, or the larger, dodecahedrally coordinated A-sites, mainly depending on their ionic radii. The large ionic radius group prefers to incorporate into Ba sites, while the small ionic radius group usually incorporates into Ti sites. The intermediate ionic radius group can occupy one of the two sites depending upon the A/B (Ba/Ti) ratio, and thermodynamic conditions, such as the partial pressure of oxygen in the sintering atmosphere [18]. The rare-earths ions (as well as Y^{3+}) have ionic radii between the Ba^{2+} (A-sites, coordination 12) and Ti^{4+} (B-sites, coordination 6) and can occupy both cationic lattice sites in the $BaTiO_3$ structure [18, 19].

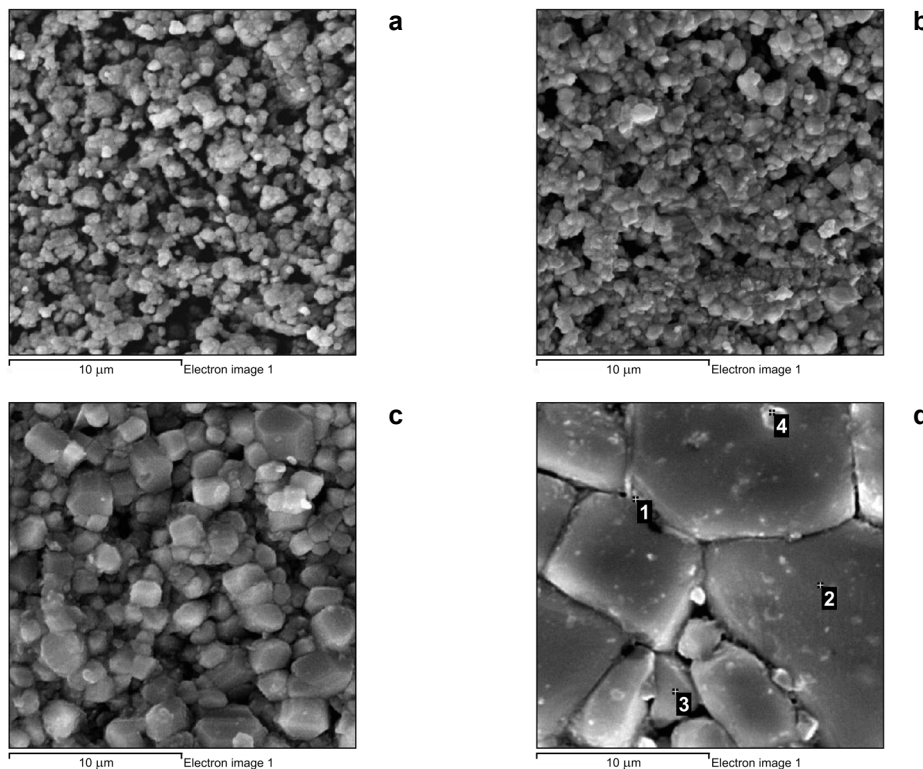
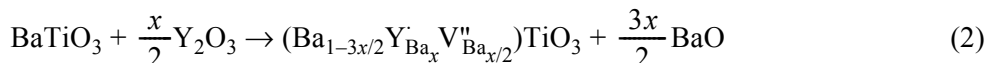
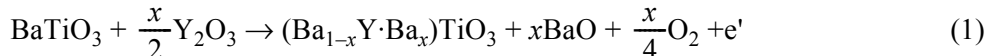


Fig. 4. SEM images of Y-doped $Ba_{0.3}Sr_{0.7}TiO_3$ specimens sintered at different temperatures for 1 h.

MAKOVEC *et al.* [20] reported that the incorporation site of Y^{3+} ion in the BaTiO_3 perovskite structure depended mainly on the starting composition. In the TiO_2 -rich samples, a relatively low concentration (below ~ 1.5 mol%) of Y^{3+} is incorporated preferentially at the Ba^{2+} lattice sites at 1400°C . In BaO -rich samples, a high solid solubility (~ 15 mol%) of Y^{3+} at the Ti^{4+} lattice sites appeared at 1500°C .

The Y^{3+} ion incorporated at the Ba^{2+} site would act as a donor, and under equilibrium conditions this extra donor charge is compensated for by ionized Ba and electronically according to the following equations (A-site substitution):



Furthermore, the Y^{3+} ion incorporated at the Ti^{4+} site acts as an acceptor, and the extra charge is compensated for by ionized oxygen vacancies according to the following equation (B-site substitution):

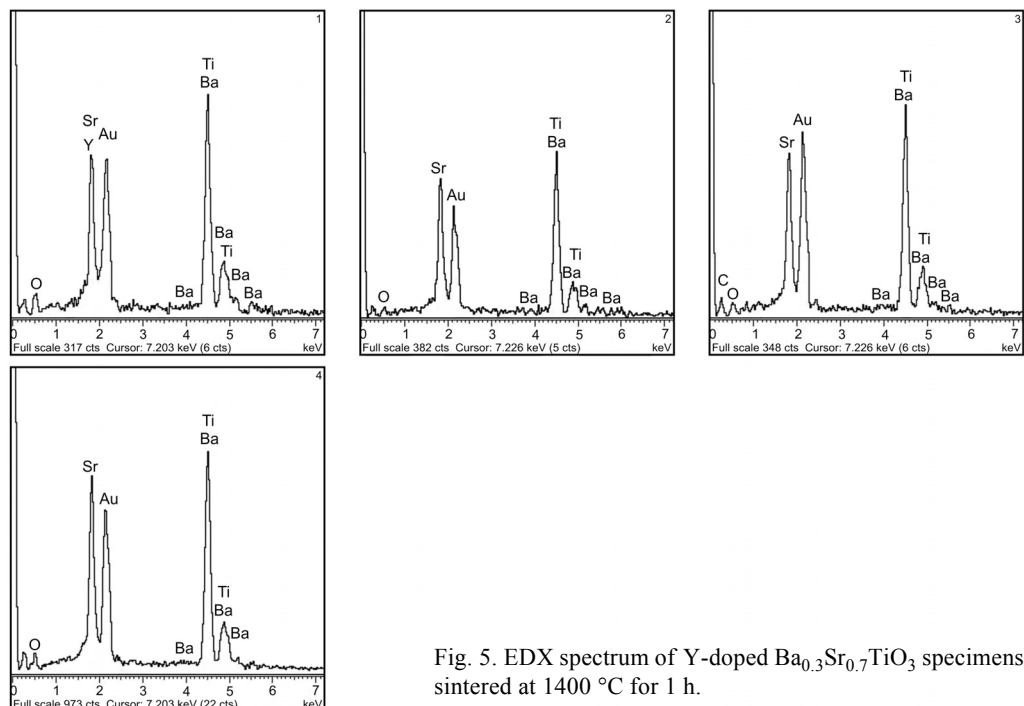
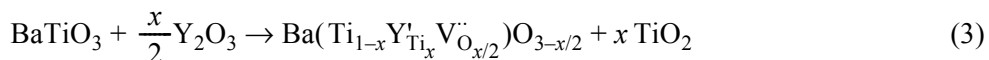


Fig. 5. EDX spectrum of Y-doped $\text{Ba}_{0.3}\text{Sr}_{0.7}\text{TiO}_3$ specimens sintered at 1400°C for 1 h.

Table. The relative elements atomic proportion.

Selected points	1	2	3	4	Theoretic value
(Ba+Sr)/Ti(atomic)	1.08	1.05	0.92	1.02	1

Therefore, if Ba-rich or Ti-rich minor phases were identified, Y^{3+} occupation site could be determined. Figure 5 shows the minor phase identifications using EDX for Y-BST fired at 1400 °C. The qualitative EDX spectra show the presence of main elements (Ba, Sr, Ti) and minor addition elements (Y) but also of an artefact related to the presence of Au used for the specimen preparation in the selected region. The relative elements analysis is listed in the Table.

SHIGEKI SATO *et al.* [21] reported that Y occupied perovskite A-site under $A/B \leq 1.00$, and perovskite B-site under $A/B > 1$ using a minor phase identification. In our experiment, the theoretic value of A/B is 1. Therefore, the Y should preferentially occupy the A site. From Fig. 4, it is clear that the BST samples sintered at 1250–1300 °C show the homogeneous grains, which may be attributed to the Y^{3+} incorporated only at the A site resulting in the similar internal stress state which existed in all grains. Also for this reason, the $Ba_{0.3}Sr_{0.7}TiO_3$ can retain stable cubic structure in the 1250–1300 °C sintering temperature.

However, when the sintering temperature reaches 1400 °C, the Y^{3+} ion may occupy both A and B sites. From the Table, it is obvious that the A/B ratio of the large grains (point 2 and 4) is larger than 1, which indicates that the Y^{3+} ion incorporated at Ti sites creates the oxygen vacancies. While the A/B ratio of the small grain (point 3) is smaller than 1, it implies that the Y^{3+} ion incorporated into Ba sites creates the Ba and Sr cation vacancies. In the grain boundary regions (point 1) simultaneously exist the A site elements (Ba + Sr) and the B site element (Ti), and this also proves that the Y^{3+} ion may occupy both cationic lattice sites in the BST specimen sintered at 1400 °C.

ARMSTRONG and BUCHANAN [22] reported that internal stress existed between cores and shells and attributed this internal stress to the thermal expansion mismatch between cores and shells in individual grains. In the Y-doped BST Specimen sintered at 1400 °C, the Y^{3+} ion occupies both cationic lattice sites, and this will lead to the distinctly different stress state between the A-site substitution region and B-site substitution region, which gives rise to the abrupt structure change from cubic to tetragonal phase observed from XRD results.

Figures 6a and 6b show the temperature dependence of the dielectric constants and TCC (temperature coefficient of capacitance) curves of the Y-doped BST system, respectively. From the dielectric measurements at low frequency (1 kHz) performed over the –30 to 130 °C temperature range, the dielectric constant increases with the sintering temperature increasing. Moreover, the sample sintered at 1400 °C exhibits the highest dielectric constant and a wide transition peak from ferroelectric to paraelectric state, which is corresponding to the XRD analysis. HENNINGS *et al.* [23] proposed that internal stresses in the microstructure were the major cause of the observed distribution of the Curie temperature. Therefore, the sample sintered at

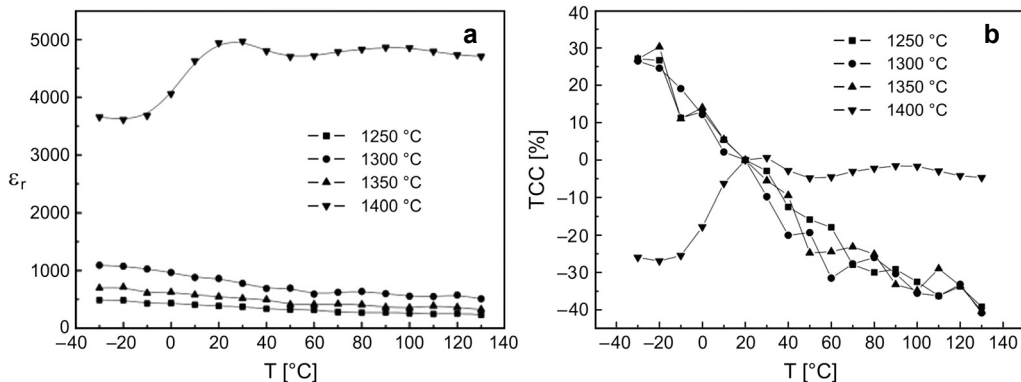


Fig. 6. Temperature variation of the dielectric constant of Y-doped Ba_{0.3}Sr_{0.7}TiO₃ specimens at different sintering temperatures for 1 h, measured at 1 kHz (a). TCC (%) curves of Y-doped Ba_{0.3}Sr_{0.7}TiO₃ as a function of different sintering temperatures for 1 h (b).

1400 °C exhibits a diffuse phase transition and this is compatible with the above analytical result.

Figure 6b shows the TCC curves of Y-doped BST as a function of sintering temperature. From the TCC curves, it can be observed that the TCC values of the samples sintered at 1250–1350 °C change much during the test temperature range. In contrast, the specimen sintered at 1400 °C has a more stable capacitance variation. The dielectric constants change within ±6% of the room temperature value over the temperature range from 10 to 130 °C.

4. Conclusions

In summary, the Y-doped Ba_{1-x}Sr_xTiO₃ ceramics were prepared by solid-state reaction and by sintering at 1250, 1300, 1350, and 1400 °C, with strontium content $x = 0.1, 0.2, 0.4, 0.7$. The increasing concentration of Sr has the following effects: *i*) decreases the grain size; *ii*) decreases considerably the ferroelectric transition temperature; and *iii*) increases the diffuse phase transition. The grain size and the microstructure density were found to increase with higher sintering temperature. The Ba_{0.3}Sr_{0.7}TiO₃ specimen sintered at 1400 °C shows exaggerated grain growth and abrupt structure change from cubic to tetragonal, which may be due to the Y³⁺ ions incorporated into both sites of BST resulting in a large stress distinction. The Ba_{0.3}Sr_{0.7}TiO₃ sintered at 1400 °C presents a more stable TCC value within ±6% over the test temperature.

Acknowledgements – The authors would like to thank for the support of Natural Science Foundation of China (No. 50872102), the Key Grant Project of Chinese Ministry of Education (No. 309022), the program for New Century Excellent Talents in University (No. NCET-08-0808) and the Chenguang Science Plan of Wuhan (No. 200750731268).

References

- [1] ANDRICH E., *Properties and applications of PTC thermistors*, Electron. Appl. **26**, 1965, pp. 123–144.
- [2] KUMAGAI S., WAKINO K., ANDO A., KITAZAWA T., *Novel evaluation method for complex high permittivity of $BaTiO_3$ families at microwave frequency*, Journal of the European Ceramic Society **26**(10–11), 2006, pp. 1817–1820.
- [3] HARI SINGH NALWA, *Handbook of Low and High Dielectric Constant Materials and Their Applications*, Academic Press, New York, Vol. 2, 1999, pp. 533–539.
- [4] GERVAIS F., CALES B., ODIER P., *Characterization of strontium titanate ceramics by infrared reflectivity spectroscopy and electron paramagnetic resonance*, Materials Research Bulletin **22**(12), 1987, pp. 1629–1633.
- [5] ROEDER R.K., SLAMOVICH E.B., *Stoichiometry control and phase selection in hydrothermally derived $Ba_xSr_{1-x}TiO_3$ powders*, Journal of the American Ceramic Society **82**(7), 1999, pp. 1665–1675.
- [6] KISHI H., MIZUNO Y., CHAZONO H., *Base-metal electrode-multilayer ceramic capacitors: Past, present and future perspectives*, Japanese Journal of Applied Physics **42**(1), 2003, pp. 1–15.
- [7] YIH-CHIEN CHEN, PING-CHOU CHEN, SHUN-CHUNG WANG, SHOU-ZHUANG LIN, *Curve fitting of dielectric constant and loss factor of ZrO_2 -doped barium strontium titanate for application in phased array antennas*, Japanese Journal of Applied Physics **46**(9A), 2007, pp. 5889–5893.
- [8] ALEXANDRU H.V., BERBECARU C., STANCULESCU F., IOACHIM A., BANCIU M.G., TOACSEN M.I., NEDELCU L., GHETU D., STOICA G., *Ferroelectric solid solutions (Ba, Sr) TiO_3 for microwave applications*, Materials Science and Engineering B **118**(1–3), 2005, pp. 92–96.
- [9] SHI-MEI SU, LIANG-YING ZHANG, HONG-TAO SUN, XI YAO, *Preparation of porous $BaTiO_3$ PTC thermistors by adding graphite porosifiers*, Journal of the American Ceramic Society **77**(8), 1994, pp. 2154–2156.
- [10] JAFFE B., COOK W.R., JAFFE H., *Piezoelectric Ceramics*, Academic Press Ltd. Reported by R.A.N. Publishers, Marietta, Ohio, 1971.
- [11] LEMANOV V.V., SMIRNOVA E.P., SYRNIKOV P.P., TARAKANOV E.A., *Phase transitions and glasslike behavior in $Sr_{1-x}Ba_xTiO_3$* , Physical Review B **54**(5), 1996, pp. 3151–3157.
- [12] LIQIN ZHOU, VILARINHO P.M., BAPTISTA J.L., *Dependence of the structural and dielectric properties of $Ba_{1-x}Sr_xTiO_3$ ceramic solid solutions on raw material processing*, Journal of the European Ceramic Society **19**(11), 1999, pp. 2015–2020.
- [13] BUSAGLIA V., BUSAGLIA M.T., VIVIANI M., MITOSERIU L., NANNI P., TREFILETTI V., PIAGGIO P., GREGORA I., OSTAPCHUK T., POKORNÝ J., PETZELT J., *Grain size and grain boundary-related effects on the properties of nanocrystalline barium titanate ceramics*, Journal of the European Ceramic Society **26**(14), 2006, pp. 2889–2898.
- [14] YUANLIANG LI, YUANFANG QU, *Substitution preference and dielectric properties of Y^{3+} -doped $Ba_{0.62}Sr_{0.38}TiO_3$ ceramics*, Materials Chemistry and Physics **110**(1), 2008, pp. 155–159.
- [15] SHIGEKI SATO, YUKIE NAKANO, AKIRA SATO, TAKESHI NOMURA, *Effect of Y-doping on resistance degradation of multilayer ceramic capacitors with Ni electrodes under the highly accelerated life test*, Japanese Journal of Applied Physics **36**(9B), 1997, pp. 6016–6020.
- [16] CHATTOPADHYAY S., AYYUB P., PALKAR V.R., MULTANI M., *Size-induced diffuse phase transition in the nanocrystalline ferroelectric $PbTiO_3$* , Physical Review B **52**(18), 1995, pp. 13177–13183.
- [17] CROSS L.E., *Relaxorferroelectrics: An overview*, Ferroelectrics **151**(1), 1994, pp. 305–320.
- [18] TSUR Y., DUNBAR T.D., RANDALL C.A., *Crystal and defect chemistry of rare earth cations in $BaTiO_3$* , Journal of Electroceramics **7**(1), 2001, pp. 25–34.
- [19] SHANNON R.D., *Revised effective ionic radii and systematic studies of interatomic distances in halides and chalcogenides*, Acta Crystallographica Section A **32**(5), 1976, pp. 751–767.
- [20] MAKOVEC D., SAMARDZIJA Z., DROFENIK M., *Solid solubility of holmium, yttrium, and dysprosium in $BaTiO_3$* , Journal of the American Ceramic Society **87**(7), 2004, pp. 1324–1329.

- [21] SHIGEKI SATO, YUKIE NAKANO, AKIRA SATO, TAKESHI NOMURA, *Mechanism of improvement of resistance degradation in Y-doped BaTiO₃ based MLCCs with Ni electrodes under highly accelerated life testing*, Journal of the European Ceramic Society **19**(6–7), 1999, pp. 1061–1065.
- [22] ARMSTRONG T.R., BUCHANAN R.C., *Influence of core-shell grains on the internal stress state and permittivity response of zirconia-modified barium titanate*, Journal of the American Ceramic Society **73**(5), 1990, pp. 1268–1273.
- [23] HENNINGS D., SCHNELL A., SIMON G., *Diffuse ferroelectric phase transitions in Ba(Ti_{1-y}Zr_y)O₃ ceramics*, Journal of the American Ceramic Society **65**(11), 1982, pp. 539–544.

Received March 6, 2009